School of Pharmacy[1], Shaanxi University of Chinese Medicine; Institute of Materia Medica[2], Key Laboratory of Gastrointestinal Pharmacology of Chinese Materia Medica of the State Administration of Traditional Chinese Medicine, School of Pharmacy, Air Force Medical University; Central Laboratory of Xi'an No. 1 Hospital[3]; Department of Neurosurgery[4], Xijing Institute of Clinical Neuroscience, Air Force Medical University, Xi'an, P. R. China

CN-3 induces mitochondrial apoptosis in glioma via Ros-mediated PI3K/AKT pathway

Yu-Ye Xue[1,#], Yun-Yang Lu[2,#], Guang-Qiang Sun[1,#], Fei Fang[3], Yu-Qiang Ji[3], Hai-Feng Tang[1,2*], Peng-Cheng Qiu[2,*], Guang Cheng[4,*]

Received January 28, 2021, accepted February 26, 2021

**Corresponding authors: Hai-Feng Tang, Peng-Cheng Qiu, Institute of Materia Medica, School of Pharmacy, Air Force Medical University, Xi'an 710032, P. R. China.*
tanghaifeng71@163. com; qpc023@126. com
Guang Cheng, Department of Neurosurgery, Xijing Institute of Clinical Neuroscience, Air Force Medical University, Xi'an, 710032, P. R. China.
chg16801@126. com
[#]These authors contributed equally to this work.

Pharmazie 76: 208-214 (2021) *doi: 10.1691/ph.2021.1363*

Recently we isolated CN-3, a new asterosaponin from starfish *Culcita novaeguineae*, and reported that asterosaponin arrests glioma cell cycle via SCUBE3. However, the multiple mechanisms underlying CN-3 anti-glioma action remains poorly known. Thus, the focus of this study was to evaluate the inhibitory effect of CN-3 on human glioma cells and its underlying molecular mechanisms. U87 and U251 cells were incubated with various concentrations of CN-3, and CCK-8, transmission electron microscopy, ICELLigence, TUNEL, flow cytometry, *N*-acetyl-L-cysteine, and western blot were conducted. As a result, it was found that CN-3 significantly inhibited U87 and U251 cell viability and proliferation in a time- and dose- dependent manner, and also induced mitochondrial apoptosis. Furthermore, we detected that CN-3 downregulated PI3K, P-Akt, AKT and BCL-2, and upregulated cytochrome C and BAX in U87 and U251 cells. Moreover, ROS triggered the inhibition and cell apoptosis for CN-3 via inactivation of P-Akt and activation of cytochrome C. In conclusion, these findings suggest that CN-3 may be a promising candidate for the development of a therapy of glioma.

1. Introduction

Glioma is the most lethal primary tumor of the central nervous system, accounting for about 80% of malignant brain tumors (Zhou et al. 2015, Huang et al. 2017). The survival rate in patients with glioma is low, and with a median survival of about 14 months (Prados et al. 2009). The current treatment strategy for malignant glioma is surgical resection followed by radiotherapy and chemotherapy (Zuo et al. 2019). However, the overall survival of patients has not improved significantly (Ding et al. 2020). Therefore, there is an urgent need to develop new effective chemotherapy drugs for glioma. Natural products are important sources for the discovery and development of new medicines (Fang et al. 2014; Huang et al. 2014; Zhang et al. 2018), and saponins have been reported to have significant anti-cancer activities (Zong et al. 2016) including those isolated from *Anemone tomentosa* (Wang et al. 2013), *Clematis argentilucida* (Zhao et al. 2014), *Anemone taipaiensis* (Wang et al. 2011; Li et al. 2013; Wang et al. 2013; Ji et al. 2016), *Ardisia pusilla* (Lin et al. 2008; Tang et al. 2009), starfish *Culcita novaeguineae* (Cheng et al. 2006) and sea cucumbers (Wu et al. 2006a, b; Zhang et al. 2006; Sun et al. 2007; Wu et al. 2007). Recently, we isolated CN-3, a new asterosaponin, from starfish *Culcita novaeguineae*, and reported that the asterosaponin arrests glioma cell cycle via SCUBE3 (Qiu et al. 2020). Saponins could induce remarkable apoptosis to glioma, but we know little about whether CN-3 could induce apoptosis in cancer, especially in glioma. Thus, we continue to discuss the anti-cancer effect and mechanism of CN-3 on U87 and U251 cells, indicating that CN-3 induces apoptosis of glioma cell lines via ROS-mediated P-Akt and cytochrome C pathways.

2. Investigations and results

2.1. CN-3 inhibited glioma cell proliferation in a dose- and time-dependent manner

CN-3 is as white, amorphous powder which gives positive Liebermann-Burchard and Molish tests. The structure of CN-3 is shown in Fig. 1A. To detect the effect of CN-3 on the proliferation of glioma cells, CCK8 and ICELLigence system were used. U87 and U251 cells were each treated with different doses of CN-3 (20, 10, 5, 2.5, 1.25, 0.625, 0.3125, 0. 15625 and 0.078125 μg/ml) for 24 h. CCK8 shows the IC_{50} values of CN-3 inhibited U87 and U251 were 1.124 μg/mL and 1.5 μg/mL, respectively (Fig. 1B). A real-time cell analysis method ICELLigence was used to measure the cell proliferation. According to the IC_{50} values, 3 μg/mL CN-3 was used as high dose, and 1.5 μg/mL CN-3 was used as low dose (Fig. 1C). The results confirmed that CN-3 had anti-proliferative effects in the glioma cells in a dose-dependent and time-dependent manner.

2.2. CN-3 induced mitochondrial apoptosis in U87 and U251 cells through PI3K/Akt pathway

There is a close relationship between cell apoptosis and cell proliferation (Lankadasari et al. 2018). In order to determine the relationship between CN-3 and glioma cell apoptosis, flow cytometry assay, TUNEL, transmission electron microscopy (TEM) and Western blot were performed. Results of flow cytometry showed that both low (55.2%) and high (67.8%) doses of CN-3 could induce apoptosis in U87, and high (22.7%) dose of CN-3 could

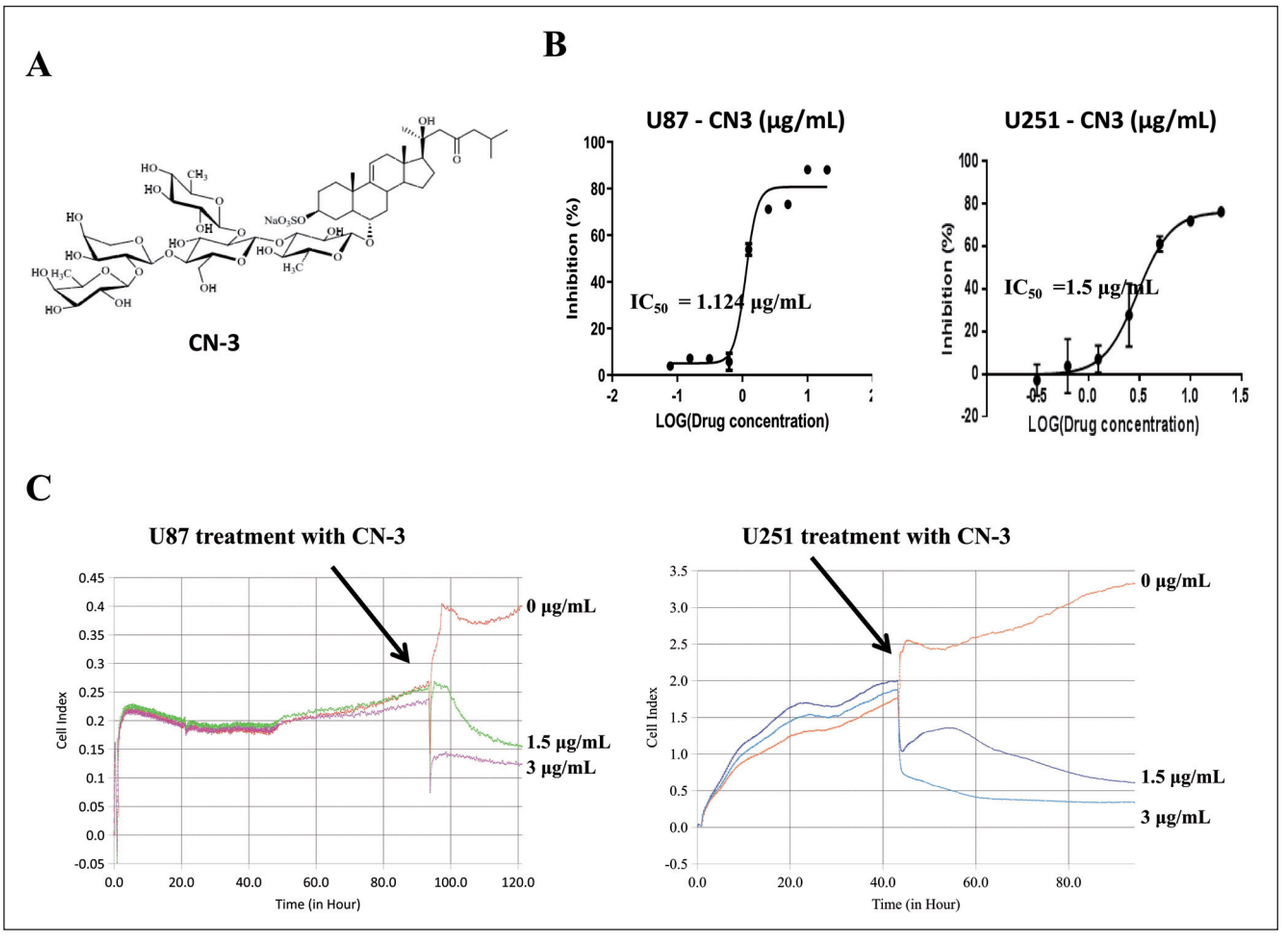

Fig. 1: CN-3 showed cytotoxicity against U87 and U251 cells in a dose- and time-dependent manner. (A) Structure of the new asterosaponin. (B) U87 and U251 cells were treated with different concentrations of CN-3 for 24 h and CCK8 assay results showed IC_{50} values of CN-3 inhibited U87 and U251 cells were 1.124 μg/mL and 1.5 μg/mL, respectively. (C) The cell growth index, recorded using ICELLigence system, showed U87 and U251 cells decreased in a short time and in a dose- and time-dependent manner when they were treated with CN-3.

induce apoptosis in U251 cells (Fig. 2A). To evaluate the degree of apoptosis in the glioma cells treated with CN-3, TUNEL staining was performed, and apoptotic cells showed green fluorescence. The result indicated that the expression of green fluorescence in the glioma cells was increased in 3 μg/mL CN-3 treated U87 and U251 cells (Fig. 2B). TEM is often used to observe typical apoptotic morphology. Phenotypic changes of U87 and U251 cells treated by CN-3 were directly observed under TEM. The cells are characterized by apoptosis, including the cytoplasmic shrinkage, the dilation of the ERs, and turgidity of the mitochondrion, the disarrangement, diminution and vacuolization (as the arrow). These features were not observed in normal glioma cells as the control group (Fig. 2C). That indicated CN-3 may induce mitochondrial apoptosis in U87 and U251 cells.

To further explore the molecular mechanism under CN-3 induced apoptosis to glioma cells, the expression of apoptosis-related proteins was evaluated by Western blot assay. After U87 and U251 cells were treated with CN-3 for 24 h, the expressions of BAX and cytochrome C were significantly increased, and PI3K, AKT, phosphorylated AKT (P-Akt) and Bcl-2 were significantly decreased (Fig. 2D). These results demonstrated that CN-3 induced mitochondrial apoptosis in U87 and U251 cells via PI3K/AKT pathway.

2.3. ROS mediated CN-3 inhibition in U87 and U251 cells via P-Akt/cytochrome C pathway

To determine whether ROS mediated CN-3-induced apoptosis, NAC, a ROS scavenger, was used to attenuate ROS generation. CCK-8 results confirmed that the CN-3 inhibition was reversed whit NAC in both U87 and U251 cells, and 8 mg/mL NAC was the optimal dose (Fig. 3A). Western blot showed NAC can significantly reverse the levels of P-Akt and cytochrome C in CN-3 treated U87 and U251 cells (Fig. 3B). These results demonstrated that ROS mediated CN-3 induced mitochondrial apoptosis in U87 and U251 cells via P-Akt/cytochrome C pathway.

3. Discussion

Malignant glioma is the most general type of primary brain tumour of the central nervous system (Wang et al. 2016), with a high incidence and mortality rate (Wu et al. 2018; Li et al. 2020). At present, the most commonly used strategy for glioma is surgical resection combined with chemotherapy and radiotherapy (Komotar et al. 2008; Jovčevska et al. 2019). However, due to the high recurrence rate of glioma, the overall cure rate of glioma is very low (Liang et al. 2020). Therefore, there is meaningful to develop new safe and effective chemotherapy drugs for glioma. Natural products are important sources of new drug development (da Silva Gomes et al. 2014; Ali et al. 2017), even against cancer (Eldhose et al. 2014; Liu and Dey 2017, Wu et al. 2020). In recent years, marine natural products were more and more recognized as a potential source of new drug candidates (van Weelden et al. 2019). Saponins have been reported to possess various anti-cancer activities (Zong et al. 2016). CN-3 is a new asterosaponin isolated from starfish *Culcita novaeguineae*. Previously, CN-3 was reported to arrest U251 cell cycle at low concentration (Qiu, Lu et al. 2020). The current study aimed to evaluate the relation between CN-3 and glioma apoptosis. We investigated the effect of CN-3 (Fig. 1A) on proliferation of glioma cells by CCK-8 and ICELLigence assays. CCK-8 showed

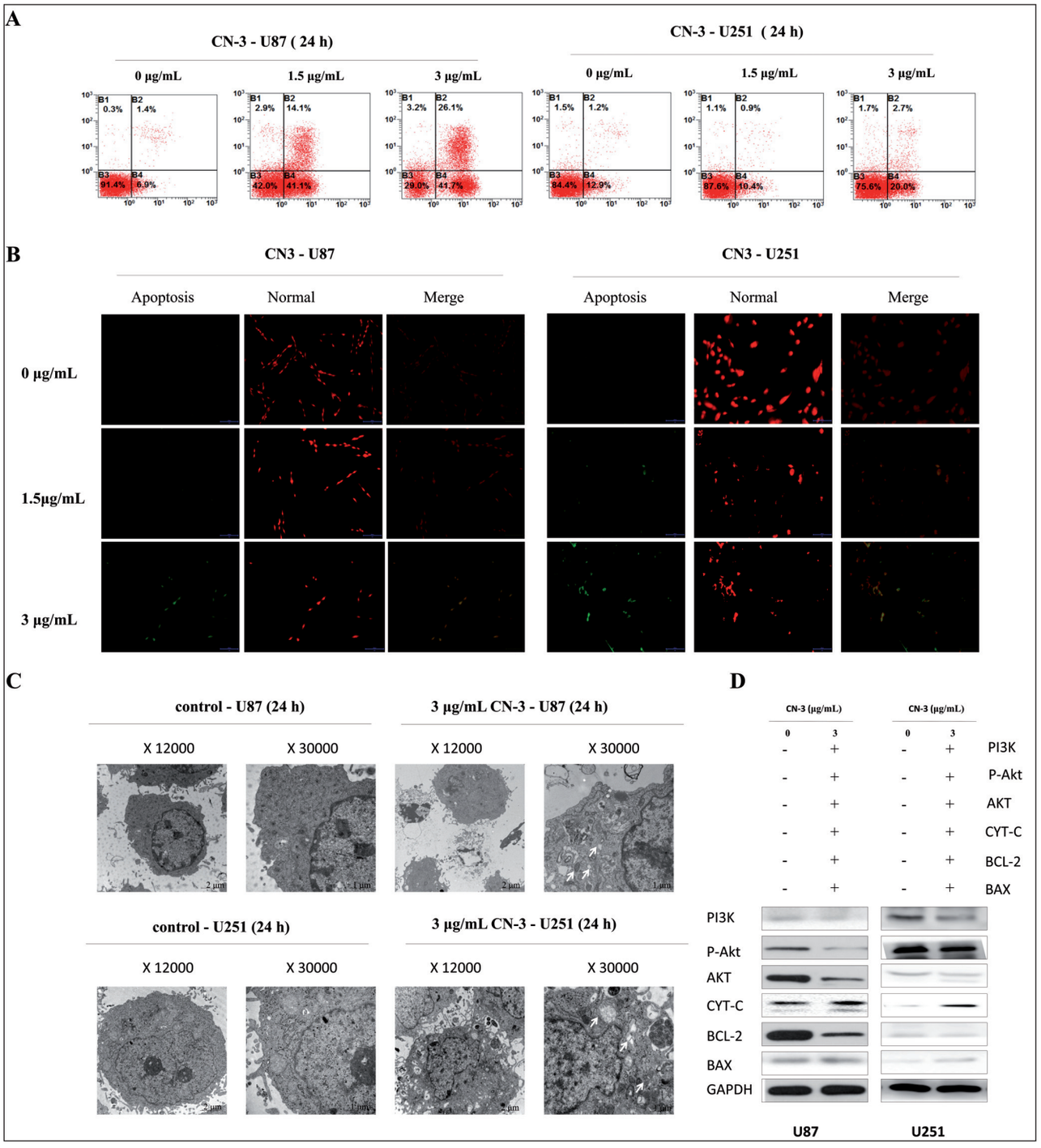

Fig. 2: CN-3 induced mitochondrial apoptosis to U87 and U251 cells. (A) Flow cytometry showed CN-3 induced apoptosis to U87 and U251 cells. (B) The apoptotic cell rates of U87 and U251 were determined using TUNEL staining assay after treatment with CN-3 (0, 1.5, 3 μg/mL) for 24 h. Green fluorescence indicates the apoptotic cells. Red fluorescence indicates both apoptotic and non-apoptotic cells. The representative pictures shown are from one of three independent experiments. (C) Some mitochondria slightly swelling and endoplasmic reticulum swelling were observed in CN3 treated U87 and U251 cells (pointed by arrows) under TEM. The representative pictures shown are from one of three independent experiments. (D) Western blot showed CN-3 increased Bax and cytochrome C, and decreased PI3K, P-Akt, AKT, and Bcl-2 in U87 and U251 cells (n = 3; "+" represents positive, and "–" represents negative).

that CN-3 significantly inhibited the cell growth of U87 and U251 cells in a dose dependent manner, and the IC_{50} values of U87 and U251 were 1.124 μg/mL and 1.5 μg/mL, respectively (Fig. 1B). Therefore 1.5 μg/mL was used as a low dose and 3 μg/mL was used as a high dose of CN-3 for treating U87 and U251 cells. ICELLigence results confirmed that CN-3 inhibited the proliferation of the U87 and U251 cells in a time- and dose-dependent manner (Fig. 1C).

Flow cytometry and TUNEL were used to detect the apoptosis of 1.5 μg/mL (low dose) or 3 μg/mL (high dose) inducing to the glioma cells. Flow cytometry showed that CN-3 could induce apoptosis in U87 (low dose: 55.2%; high dose: 67.8%) and U251 (high dose: 22.7%) cells (Fig. 2A). We used TUNEL staining to evaluate the degree of CN-3 induced apoptosis of U87 and U251 cells. Green fluorescence indicates the apoptotic cells, and red fluorescence indicates both apoptotic and non-apoptotic cells. TUNEL staining

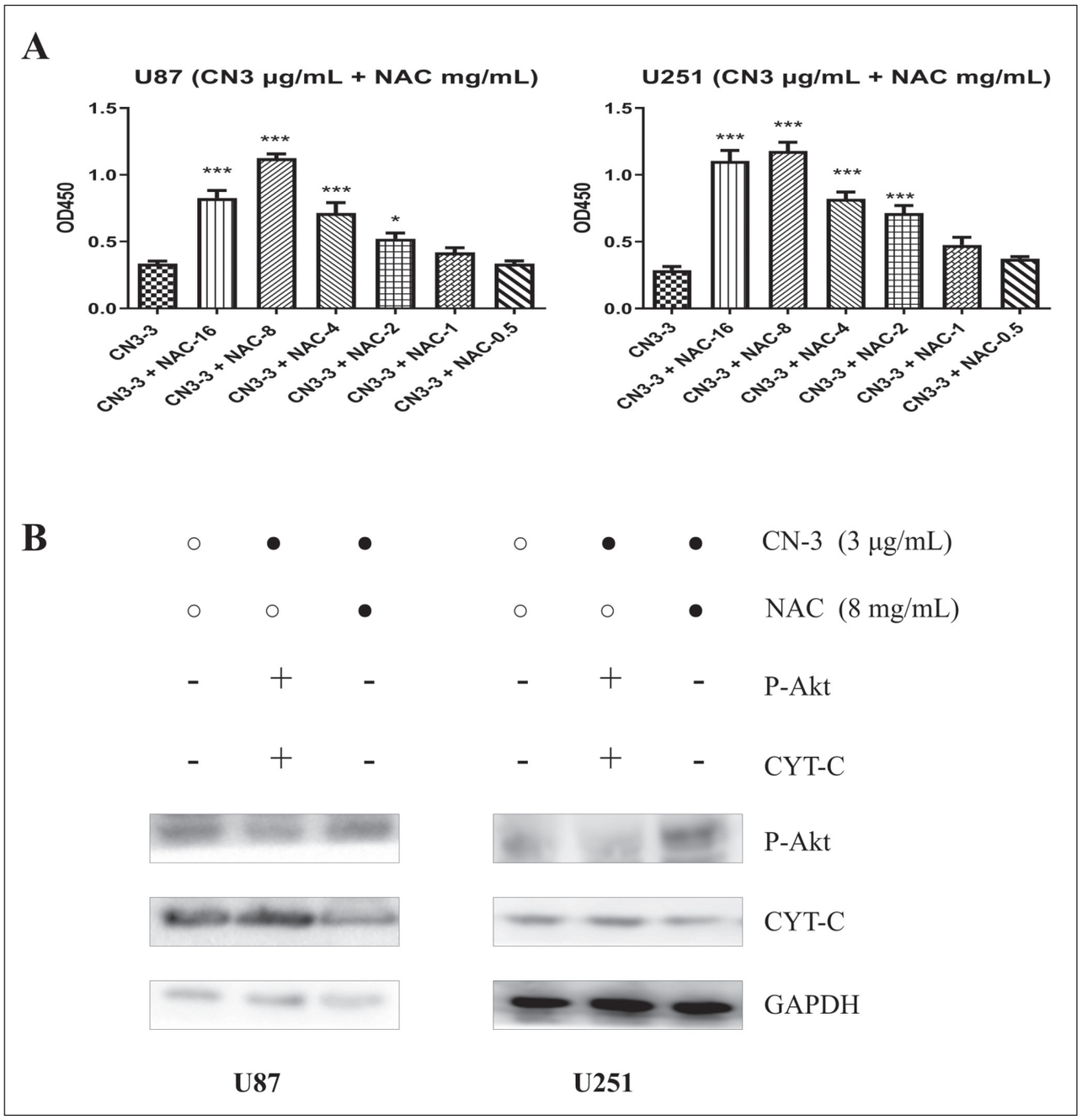

Fig. 3: CN-3 induced mitochondrial apoptosis in U87 and U251 cells through ROS-mediated activation of P-Akt/cytochrome C pathway. (A) The CCK8 assay determined that 8 mg/mL NAC was the optimal dose, in combination with CN-3 and could reverse the inhibition in U87 and U251 cells (***$p < 0.001$, as compared with CN-3 treatment alone). (B) Western blot showed CN-3 increased cytochrome C and decreased P-Akt in U87 and U251 cells, while NAC reversed the trends caused by CN-3 (n = 3; "+" represents positive, and "–" represents negative; "●" represents added, and "O" represents un-added).

showed that almost no green fluorescence was detected in U87 and U251 cells of the control group, however, the expression of green fluorescence treated with CN3-3 was significantly increased in U87 and U251 cells (Fig. 2B).

Mitochondria are the vital organelles for the regulation of the cellular apoptosis pathway. Phenotypic changes of U87 and U251 cells treated by CN-3 were directly observed under TEM. The cells are characterized by apoptosis, including the cytoplasmic shrinkage, the dilation of the ERs, and turgidity of the mitochondrion, the disarrangement, diminution and vacuolization (as the arrow). In contrast, these feature were not observed in normal glioma cells as the control group (Fig. 2C). That indicated CN-3 may induce mitochondrial apoptosis in U87 and U251 cells. This is consistent with the observation of TUNEL staining, and indicated CN-3 may issue in mitochondrial apoptosis in U87 and U251 cells. Studies have shown that induction of tumor cell apoptosis is an effective way to treat patients (Che et al. 2018; Yang et al. 2019; Pitucha et al. 2020). Curcumin induces cancer cell apoptosis and inhibits tumor growth and proliferation (He et al. 2019). Mitochondrial outer membrane permeabilization (MOMP) and mitochondrial swelling are the signature feature and plays a major role in apoptosis (Geng et al. 2017). By changing mitochondrial membrane permeability, the drug induce the release of cytochrome C and the activation of caspase-3, thus leading to mitochondrial apoptosis (Bai et al. 2017; Reheman et al. 2020). Bcl-2 family is an important regulator of mitochondrial apoptosis (Zhao et al.

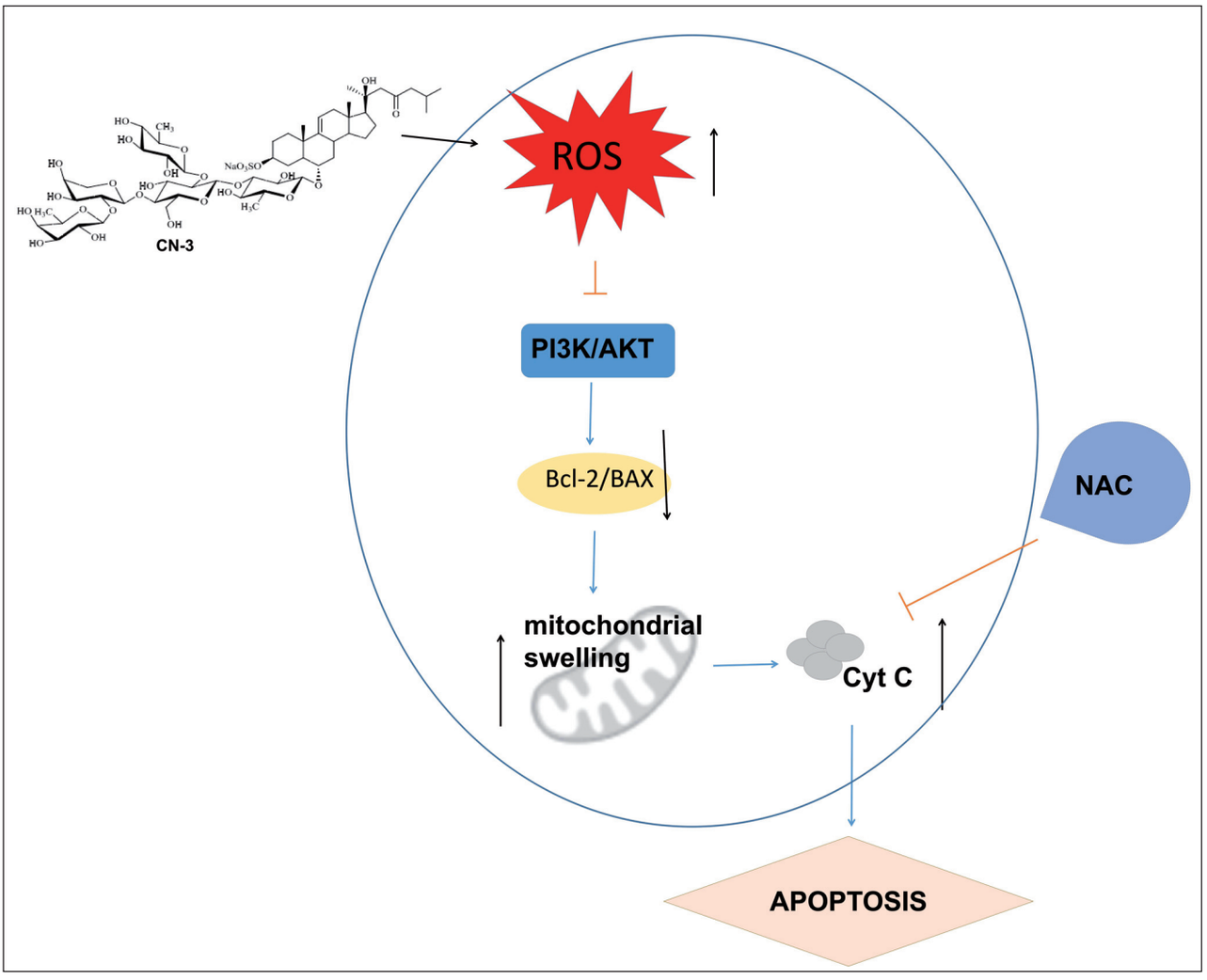

Fig. 4: Schematic illustration of CN-3 induces ROS-dependent apoptosis in U87 and U251.

2016; Jiang et al. 2018). Bcl-2 promotes cell survival by stabilizing mitochondria and endoplasmic reticulum, while BAX inhibits cell survival (Yin et al. 2017; Hussain et al. 2018). The PI3K-AKT pathway played an critical role in regulating cell growth and apoptosis (Xu et al. 2012). P-Akt inhibited Bad and Bax and increased the expression of Bcl-2 in BCL family members (Li et al. 2020). In our study, western blot showed that CN-3 downregulated PI3K, P-Akt, AKT and BCL-2 and upregulated cytochrome C and BAX in U87 and U251 cells (Fig. 2D). Those indicated that CN-3 downregulated PI3K/AKT pathway to induce mitochondrion turgidity and cytochrome C release, which triggered cell death, thus leading to mitochondrial apoptosis.

The generation of reactive oxygen species plays an important role in signaling pathway activation and apoptosis (Wang et al. 2008; Tang et al. 2014). Excessive ROS leads to mitochondrial swelling and MOMP of mitochondria-mediated apoptosis by inducing the release of cytochrome C (Li et al. 2014, 2018). To investigate the role of ROS in mitochondrial apoptosis induced by CN3 in glioma cells U87 and U251, we used reactive oxygen scavenger N-acetyl cysteine (NAC). Studies have reported that natural products generate ROS to induce apoptosis, like dioscin in cervical carcinoma HeLa and SiHa Cells through ROS-mediated DNA damage and the mitochondrial signaling pathway (Zhao et al. 2016). Nanoparticle delivery of curcumin induces cellular hypoxia and ROS-mediated apoptosis via modulation of Bcl-2 in human neuroblastoma (Pan et al. 2018). Previously, we found that ROS mediated the apoptosis induced by a steroidal saponin from *Paris vietnamensis* (Takht.) in U87R (Pan et al. 2018). In this study, the reactive oxygen scavenger NAC was used, and the results showed that NAC reduced CN-3 induced apoptosis, and ROS mediated the inhibitory effect of CN-3 on U87 and U251 cells (Fig. 3A). AKT is activated by phosphorylation and P-Akt is as the key factor in PI3K/AKT pathway (Li 2020). Cytochrome C release is the result of mitochondrial swelling and triggered cell death (Bai et al. 2017; Reheman et al. 2020). Western blot was used to investigate the mechanism of NAC reversing the inhibition of CN-3 in the mitochondrial apoptosis. The results showed that NCA reversed the upregulation levels of cytochrome C and downregulation levels of P-Akt caused by CN-3 (Fig. 3B). This suggests that CN-3 induced glioma cells U87 and U251 mitochondrial apoptosis via ROS-mediated inactivation of P-Akt and activation of cytochrome C.

Our results showed that CN-3 induced mitochondrial apoptosis to U87 and U251 cells through PI3K/AKT pathway. That ROS-mediated inactivation of P-Akt and activation of cytochrome C triggered the mitochondrial apoptosis caused by CN-3 (Fig. 4). This suggested that CN-3 may be an effective chemotherapeutic agent for the inhibition of proliferation and induction of apoptosis in glioma cells.

4. Experimental

4.1. Cell culture

Human glioma cell lines U87 and U251 were obtained from the Cell Bank of Chinese Academy of Science (Shanghai, China). The cell lines were cultured in DMEM

(Corning, Beijing, China) supplemented with 10% FBS (Ausbian, Harbin, China), maintained at 37 °C with 5% CO_2. The medium was changed every three days.

4.2. Cell proliferation assay

The logarithmic phase cells were cultured in 96-well plates at density of 5×10^3 cells/well, and treated with different doses (20, 10, 5, 2.5, 1.25, 0.625, 0.3125, 0.15625, 0.078125 μg/ml) of CN-3 for 24 h, four replicated wells were set for each experimental condition. Cell proliferation and cytotoxicity were assessed using Cell Counting Kit-8 (CCK-8), 10 μl CCK-8 was added to each well and incubated at 37 °C and 5% CO_2 for 2 h, measuring the absorbance at wavelength of 450 nm using a microplate reader.

4.3. Flow cytometric analysis

The logarithmic phase cells were cultured at 6-well plates at density of 2×10^5 cells, were treated with different doses (0, 1.5, 3 μg/ml) of CN-3 for 24 h, three replicated wells were used for each experimental condition. Then the treated cells were digested with trypsin and washed in cold PBS (4 °C) twice, cells apoptosis was determined using Annexin V Apoptosis Detection kit I. The result was evaluated by a flow cytometer (BD Bioscience) after the cells were labeled with Annexin-V and PI.

4.4. Transmission electron microscopy analysis

Cells were fixed in 2% glutaraldehyde for 2 h and washed two times with PBS for 10 min. Then fixed in 1% OsO_4 for 2 h. After gradient dehydration with ethanol, the cells were embedded in epoxy resin and cut into 50-60 nm sections. The sections were stained with uranyl acetate combined with lead citrate. Samples were cut and analyzed with a JEM-1400 transmission electron microscope (JEM-1400, JEOL, Japan).

4.5. TUNEL assay

Cells were cultured on cell plates coated with poly-L-lysine (PLL) and incubated for 24 h. After incubation with CN-3 for 24 h, and PBS washing twice, the cells were incubated with fluorescein isothiocyanate (FITC)-dUTP for 15 min at room temperature in the dark. Thereafter, the cells were washed additional two times with PBS. Then, under a fluorescence microscope five random fields of vision were inspected, while apoptotic cells (green fluorescence cells) and normal cells (red fluorescence cells) were recorded.

4.6. Real time cellular analysis (RTCA)

The proliferation assay and the cell growth index were recorded using ICELLigence (ACEA Biosciences, Inc., San Diego, CA, USA) as the real time cell analysis (RTCA) system. All monitoring was performed at 37 °C with regulated CO_2 content 5%. E-plates (culture plates for the ICELLigence system) containing 200 μl culture medium per well were equilibrated to 37 °C, the cells were seeded at 5000 cells per well in cell culture.

4.7. Western blot analysis

Cells were treated with different doses (0, 3 μg/ml) of CN-3 for 24 h, and washed twice in cold PBS. Then the treated cells were collected and lysed in RIPA lysis buffer. Bicinchoninic acid (BCA) kit was used to determine protein concentration, all the protein samples were quantified to be the same concentration. Cell lysates (50 μg) were subjected to sodium dodecyl sulfate (SDS)-polyacrylamide gel electrophoresis (PAGE) and transferred onto polyvinylidene difluoride (PVDF) membrane. Then incubated with the primary antibody anti-PI3K (proteintech Inc, China, product code: 20584-1-AP), anti-P-Akt (Affinity Biosciences, Inc., USA, product code: AF0908), anti-AKT (Servicebio Inc., China, product code: GB13427), anti-BAX (Servicebio Inc., China, product code: GB11690), anti-cytochrome C (Servicebio Inc., China, product code: GB11080), anti-BCL2 (Wanleibio Co, China, product code: WL0234), and anti-GAPDH (Santa Cruz Biotechnology, Inc., USA, product code: sc-32233) at 4°C overnight after blocked with 5% non-fat dry milk, wash with 0. 1% PBST for 3 times for 5 minutes each time, and then incubated again with the secondary antibody in a dark place for 1 h, and repeat the washing process. The protein level was corrected using glyceraldehyde-3-phosphate dehydrogenase (GAPDH). The band density was quantified by densitometry using Image J software.

4.8. Statistical analysis

Results presented were analyzed by the GraphPad Prism software 7. 0, and all the data were expressed as mean±standard deviation, and the one-way Analysis of Variance (ANOVA) was used to analyze the multigroup differences. A t test was used to examine the differences between two groups. The value of $p < 0.05$ suggested that the difference was statistically significant differences.

Conflicts of interest: The authors declare that there is no conflict of interest regarding the publication of this paper

Funding Statement: This research was funded by National Natural Science Foundation of China (No. 81973192, 81903862, and 81473132), Social R&D Program of Shaanxi Province (No. 2020SF-311 and 2021SF-388) and Shaanxi Provincial Administration of Traditional Chinese Medicine (No. 2019-ZZ-JC015).

References

Ali L, Khan AL, Al-Broumi M, Al-Harrasi R, Al-Kharusi L, Hussain J, Al-Harrasi A (2017) New enzyme-inhibitory triterpenoid from marine macro brown alga Padina boergesenii Allender & Kraft. Mar Drugs 15: 19.

Bai D, Yu S, Zhong S, Zhao B, Qiu S, Chen J, Lunagariya J, Liao X, Xu S (2017) d-Amino acid position influences the anticancer activity of galaxamide analogs: an apoptotic mechanism study. Int J Mol Sci 18: 544.

Che Y, Li J, Li Z, Li J, Wang S, Yan Y, Zou K, Zou L (2018) Osthole enhances antitumor activity and irradiation sensitivity of cervical cancer cells by suppressing ATM/NF-κB signaling. Oncol Rep 40: 737–747.

Cheng G, Zhang X, Tang HF, Zhang Y, Zhang XH, Cao WD, Gao DK, Wang XL, Jin BQ (2006) Asterosaponin 1, a cytostatic compound from the starfish Culcita novaeguineae, functions by inducing apoptosis in human glioblastoma U87MG cells. J Neurooncol 79: 235-241.

da Silva Gomes EC, Jimenez GC, da Silva LC, de Sá FB, de Souza KP, Paiva GS, de Souza IA (2014) Evaluation of antioxidant and antiangiogenic properties of caesalpinia echinata extracts. J Cancer 5: 143-150.

Ding P, Liang B, Shou J, Wang X (2020) lncRNA KCNQ1OT1 promotes proliferation and invasion of glioma cells by targeting the miR-375/YAP pathway. Int J Mol Med 46: 1983–1992.

Eldhose B, Gunawan M, Rahman M, Latha MS, Notario V (2014) Plumbagin reduces human colon cancer cell survival by inducing cell cycle arrest and mitochondria-mediated apoptosis. Int J Oncol 45: 1913-1920.

Fang SM, Wu CJ, Li CW, Cui CB (2014) A practical strategy to discover new antitumor compounds by activating silent metabolite production in fungi by diethyl sulphate mutagenesis. Mar Drugs 12: 1788-1814.

Geng Y, Zhou Y, Wu S, Hu Y, Lin K, Wang Y, Zheng Z, Wu W (2017) Sulforaphane induced apoptosis via promotion of mitochondrial fusion and ERK1/2-mediated 26S proteasome degradation of novel pro-survival Bim and upregulation of Bax in human non-small cell lung cancer cells. J Cancer 8: 2456–2470.

He YC, He L, Khoshaba R, Lu FG, Cai C, Zhou FL, Liao DF, Cao D (2019) Curcumin nicotinate selectively induces cancer cell apoptosis and cycle arrest through a p53-mediated mechanism. Molecules 24: 4179.

Huang, L., T. Zhang, S. Li, et al. (2014). " Huang L, Zhang T, Li S, Duan J, Ye F, Li H, She Z, Gao G, Yang X (2014) Anthraquinone G503 induces apoptosis in gastric cancer cells through the mitochondrial pathway. PLoS One 9: e108286.

Huang YT, Zhang Y, Wu Z, Michaud DS (2017) Genotype-based gene signature of glioma risk. Neuro Oncol 19: 940–950.

Hussain SS, George S, Singh S, Jayant R, Hu CA, Sopori M, Chand HS (2018) A small molecule BH3-mimetic suppresses cigarette smoke-induced mucous expression in airway epithelial cells. Sci Rep 8: 13796.

Ji CC, Tang HF, Hu YY, Zhang Y, Zheng MH, Qin HY, Li SZ, Wang XY, Fei Z, Cheng G (2016) Saponin 6 derived from Anemone taipaiensis induces U87 human malignant glioblastoma cell apoptosis via regulation of Fas and Bcl-2 family proteins. Mol Med Rep 14: 380–386.

Jiang W, Wang R, Liu D, Zuo M, Zhao C, Zhang T, Li W (2018) Protective effects of kaempferitrin on advanced glycation end products induce mesangial cell apoptosis and oxidative stress. Int J Mol Sci 19: 3334.

Jovčevska I, Zottel A, Šamec N, Mlakar J, Sorokin M, Nikitin D, Buzdin AA, Komel R (2019) High *FREM2* gene and protein expression are associated with favorable prognosis of *IDH*-WT glioblastomas. Cancers 11: 1060.

Komotar RJ, Otten ML, Moise G, Connolly ES Jr. (2008) Radiotherapy plus concomitant and adjuvant temozolomide for glioblastoma-a critical review. Clin Med Oncol 2: 421–422.

Lankadasari MB, Aparna JS, Mohammed S, James S, Aoki K, Binu VS, Nair S, Harikumar KB (2018) Targeting S1PR1/STAT3 loop abrogates desmoplasia and chemosensitizes pancreatic cancer to gemcitabine. Theranostics 8: 3824–3840.

Li H, Li T, Huang D, Zhang P. Long noncoding RNA SNHG17 induced by YY1 facilitates the glioma progression through targeting miR-506-3p/CTNNB1 axis to activate Wnt/β-catenin signaling pathway. Cancer Cell Int 20: 29.

Li H, Xiao Y, Tang L, Zhong F, Huang G, Xu JM, Xu AM, Dai RP, Zhou ZG (2018) Adipocyte fatty acid-binding protein promotes palmitate-induced mitochondrial dysfunction and apoptosis in macrophages. Front Immunol 9: 81.

Li J, Tang H, Zhang Y, Tang C, Li B, Wang Y, Gao Z, Luo P, Yin A, Wang X, Cheng G, Fei Z (2013) Saponin 1 induces apoptosis and suppresses NF-κB-mediated survival signaling in glioblastoma multiforme (GBM). PLoS One 8: e81258.

Li W, Li C, Ma L, Jin F (2020) Resveratrol inhibits viability and induces apoptosis in the small-cell lung cancer H446 cell line via the PI3K/Akt/c-Myc pathway. Oncol Rep 44: 1821–1830.

Li X, Zhang M, Zhou H (2014) The morphological features and mitochondrial oxidative stress mechanism of the retinal neurons apoptosis in early diabetic rats. J Diabetes Res 2014: 678123.

Liang J, Lv X, Lu C, Ye X, Chen X, Fu J, Luo C, Zhao Y (2020) Prognostic factors of patients with Gliomas - an analysis on 335 patients with Glioblastoma and other forms of Gliomas. BMC Cancer 20: 35.

Lin H, Zhang X, Cheng G, Tang HF, Zhang W, Zhen HN, Cheng JX, Liu BL, Cao WD, Dong WP, Wang P (2008) Apoptosis induced by ardipusilloside III through BAD dephosphorylation and cleavage in human glioblastoma U251MG cells. Apoptosis 13: 247–257.

Liu Y, Dey M (2017) Dietary phenethyl isothiocyanate protects mice from colitis associated colon cancer. Int J Mol Sci 18: 1908.

Pan L, Zhao Y, Farouk MH, Bao N, Wang T, Qin G (2018) Integrins were involved in soybean agglutinin induced cell apoptosis in IPEC-J2. Int J Mol Sci 19: 587.

Pitucha M, Korga-Plewko A, Kozyra P, Iwan M, Kaczor AA (2020) 2,4-Dichlorophenoxyacetic Thiosemicarbazides as a new class of compounds against stomach cancer potentially intercalating with DNA. Biomolecules 10: 296.

Prados MD, Chang SM, Butowski N, DeBoer R, Parvataneni R, Carliner H, Kabuubi P, Ayers-Ringler J, Rabbitt J, Page M, Fedoroff A, Sneed PK, Berger MS, McDermott MW, Parsa AT, Vandenberg S, James CD, Lamborn KR, Stokoe D, Haas-

Kogan DA (2009) Phase II study of erlotinib plus temozolomide during and after radiation therapy in patients with newly diagnosed glioblastoma multiforme or gliosarcoma. J Clin Oncol 27: 579–584.

Qiu PC, Lu YY, Zhang S, Li H, Bao H, Ji YQ, Fang F, Tang HF, Cheng G (2020) Reduction of SCUBE3 by a new marine-derived asterosaponin leads to arrest of glioma cells in G1/S. Oncogenesis 9: 71.

Reheman D, Zhao J, Guan S, Xu GC, Li YJ, Sun SR (2020) Apoptotic effect of novel pyrazolone-based derivative [Cu(PMPP-SAL)(EtOH)] on HeLa cells and its mechanism. Sci Rep 10: 18235.

Sun P, Liu BS, Yi YH, Li L, Gui M, Tang HF, Zhang DZ, Zhang SL (2007) A new cytotoxic lanostane-type triterpene glycoside from the sea cucumber Holothuria impatiens. Chem Biodivers 4: 450–457.

Tang HF, Yun J, Lin HW, Chen XL, Wang XJ, Cheng G (2009) Two new triterpenoid saponins cytotoxic to human glioblastoma U251MG cells from Ardisia pusilla. Chem Biodivers 6: 1443–1452.

Tang SA, Zhou Q, Guo WZ, Qiu Y, Wang R, Jin M, Zhang W, Li K, Yamori T, Dan S, Kong D (2014) In vitro antitumor activity of stellettin B, a triterpene from marine sponge Jaspis stellifera, on human glioblastoma cancer SF295 cells. Mar Drugs 12: 4200–4213.

van Weelden G, Bobiński M, Okła K, van Weelden WJ, Romano A, Pijnenborg JMA (2019) Fucoidan structure and activity in relation to anti-cancer mechanisms. Mar Drugs 17: 32.

Wang C, Zhou GL, Vedantam S, Li P, Field J (2008) Mitochondrial shuttling of CAP1 promotes actin- and cofilin-dependent apoptosis. J Cell Sci 121: 2913–2920.

Wang XY, Chen XL, Tang HF, Gao H, Tian XR, Zhang PH (2011) Cytotoxic triterpenoid saponins from the rhizomes of Anemone taipaiensis. Planta Med 77: 1550–1554.

Wang Y, Kang W, Hong LJ, Hai WL, Wang XY, Tang HF, Tian XR (2013) Triterpenoid saponins from the root of Anemone tomentosa. J Nat Med 67: 70-77.

Wang Y, Tang H, Zhang Y, Li J, Li B, Gao Z, Wang X, Cheng G, Fei Z (2013) Saponin B, a novel cytostatic compound purified from Anemone taipaiensis, induces apoptosis in a human glioblastoma cell line. Int J Mol Med. 32: 1077–1084.

Wang Z, Zhang C, Liu X, Wang Z, Sun L, Li G, Liang J, Hu H, Liu Y, Zhang W, Jiang T (2016) Molecular and clinical characterization of PD-L1 expression at transcriptional level via 976 samples of brain glioma. Oncoimmunology 5: e1196310.

Wu DM, Wang S, Wen X, Han XR, Wang YJ, Fan SH, Zhang ZF, Shan Q, Lu J, Zheng YL (2018) MircoRNA-1275 promotes proliferation, invasion and migration of glioma cells via SERPINE1. J Cell Mol Med 22: 4963–4974.

Wu J, Yi YH, Tang HF, Wu HM, Zhou ZR (2007) Hillasides A and B, two new cytotoxic triterpene glycosides from the sea cucumber Holothuria hilla Lesson. J Asian Nat Prod Res 9: 609–615.

Wu J, Yi YH, Tang HF, Wu HM, Zou ZR, Lin HW (2006) Nobilisides A - C, three new triterpene glycosides from the sea cucumber Holothuria nobilis. Planta Med. 72: 932–935.

Wu J, Yi YH, Tang HF, Zou ZR, Wu HM (2006) Structure and cytotoxicity of a new lanostane-type triterpene glycoside from the sea cucumber Holothuria hilla. Chem Biodivers 3: 1249–1254.

Wu L, Guo C, Wu J (2020) Therapeutic potential of PPARγ natural agonists in liver diseases. J Cell Mol Med 24: 2736–2748.

Xu J, Qian J, Xie X, Lin L, Zou Y, Fu M, Huang Z, Zhang G, Su Y, Ge J (2012) High density lipoprotein protects mesenchymal stem cells from oxidative stress-induced apoptosis via activation of the PI3K/Akt pathway and suppression of reactive oxygen species. Int J Mol Sci 13: 17104–17120.

Yang H, Bai X, Zhang H, Zhang J, Wu Y, Tang C, Liu Y, Yang Y, Liu Z, Jia W, Wang W (2019) Antrodin C, an NADPH dependent metabolism, encourages crosstalk between autophagy and apoptosis in lung carcinoma cells by use of an AMPK inhibition-independent blockade of the Akt/mTOR pathway. Molecules 24: 993.

Yin J, Wang B, Zhu X, Qu X, Huang Y, Lv S, Mu Y, Luo G (2017) The small glutathione peroxidase mimic 5P may represent a new strategy for the treatment of liver cancer. Molecules 22: 1495.

Zhang D, Shu C, Lian X, Zhang Z (2018) New antibacterial Bagremycins F and G from the marine-derived *Streptomyces* sp. ZZ745. Mar Drugs 16: 330.

Zhang SY, Yi YH, Tang HF, Li L, Sun P, Wu J (2006) Two new bioactive triterpene glycosides from the sea cucumber Pseudocolochirus violaceus. J Asian Nat Prod Res 8: 1–8.

Zhao M, Ma N, Qiu F, Hai WL, Tang HF, Zhang Y, Wen AD (2014) Triterpenoid saponins from the roots of Clematis argentilucida and their cytotoxic activity. Planta Med 80: 942–948.

Zhao X, Tao X, Xu L, Yin L, Qi Y, Xu Y, Han X, Peng J (2016) Dioscin induces apoptosis in human cervical carcinoma HeLa and SiHa cells through ROS-mediated DNA damage and the mitochondrial signaling pathway. Molecules 21: 730.

Zhou Y, Wu S, Liang C, Lin Y, Zou Y, Li K, Lu B, Shu M, Huang Y, Zhu W, Kang Z, Xu D, Hu J, Yan G (2015) Transcriptional upregulation of microtubule-associated protein 2 is involved in the protein kinase A-induced decrease in the invasiveness of glioma cells. Neuro Oncol 17: 1578–1588.

Zong JF, Peng YR, Bao GH, Hou RY, Wan XC (2016) Two new oleanane-type saponins with anti-proliferative activity from Camellia oleifera Abel. seed cake. Molecules 21: 188.

Zuo S, Zhang X, Wang L (2019) A RNA sequencing-based six-gene signature for survival prediction in patients with glioblastoma. Sci Rep 9: 2615.